Chapter 4

Peptide ligands for Methuselah, a *Drosophila* G protein-coupled receptor associated with extended lifespan

William W. Ja, Anthony P. West, Jr., Silvia L. Delker, Pamela J. Bjorkman, Seymour Benzer, and Richard W. Roberts

Methuselah (Mth) is a G protein-coupled receptor (GPCR) associated with extended lifespan and stress resistance in *Drosophila melanogaster*. Eight rounds of *in vitro* selection have been performed using mRNA display of a random 27-mer peptide library against the extracellular domain of Mth. Isolated peptide sequences reveal the consensus, (R/P)xxWxxR (RWR motif). Synthesized RWR motif peptides (R8-01, -12, and -14) exhibit high affinity for the Mth ectodomain (K_D = 15 to 30 nM), as determined by surface plasmon resonance. The recently identified Mth agonist, Stunted, as well as a selected non-RWR motif peptide (R8-04), both competed with R8-01 for binding to the ectodomain, indicating that this site is a "hot spot" for interaction. A low-resolution crystal structure of the Mth:R8-01 complex suggests that the peptide binds at an interface between the ectodomain and extracellular loops. Despite being selected against the immobilized ectodomain, peptides tagged with rhodamine recognize and label cells expressing full-length Mth. RWR motif peptides act as antagonists to Stunted-induced Mth signaling in a cell-based GPCR calcium mobilization assay. Furthermore, characterization of mutant variants of the selected peptides has revealed a novel, potent agonist for Mth.

Introduction

G protein-coupled receptors (GPCRs)[1] mediate cell signaling from a diverse array of extracellular ligands (e.g., light, hormones, neuropeptides, odorants, and other small molecules) to intracellular signal transduction proteins (*1*). GPCRs are defined by a seven α-helical transmembrane domain, an extracellular N-terminus, which assists in ligand recognition, and an intracellular C-terminus, which is involved in G protein coupling and signal propagation. Because of their involvement in numerous cell processes, GPCRs are the target of approximately 50% of marketed drugs and new GPCR ligands continue to be pursued and developed (*2, 3*).

Commonly used, naïve approaches toward GPCR ligand identification involve high-throughput screening of a molecular library (10^2 to 10^5 unique members) in functional, cell-based assays (*3-5*). *In vitro* selection is an alternative approach for the rapid isolation of new ligands against biological targets (*6, 7*). Large, diverse libraries of unique molecules, composed of polypeptides, nucleic acids, or small molecules, are allowed to bind to a target of interest. Non-binding members are removed and functional molecules are recovered and identified. mRNA display, where each peptide in a library is covalently linked to its encoding RNA sequence, is a selection technique that allows access to very high library complexities ($>10^{13}$) in a robust format. An mRNA display library was recently used to isolate peptides that modulate G protein signaling by affecting intracellular, heterotrimeric G proteins (*8*).

---

[1] Abbreviations: CHO, Chinese hamster ovary; FACS, fluorescence-activated cell sorting; Fmoc, Fluorenylmethoxycarbonyl; GPCR, G protein-coupled receptor; HEK, human embryonic kidney; HPLC, high performance liquid chromatography; MALDI-TOF, matrix-assisted laser desorption/ionization time-of- flight; Mth, Methuselah; SPR, surface plasmon resonance; TFA, trifluoroacetic acid.

Selection techniques have had limited success targeting GPCRs because of the difficulty in expression, solubilization, and presentation of the target (e.g., by immobilization on agarose). Several groups have performed successful selections with phage display libraries based on known ligands against cells expressing the GPCR of interest (*9-13*). Naïve phage display libraries, displaying either random peptides or antibody-based scaffolds, have also been selected against GPCRs expressed in cells (*14-17*), often producing ligands that act as antagonists with a range of affinities and/or IC_{50} values (nM to high μM). These results are tempered by several published failures where selected peptides were not receptor-specific, despite best efforts to target the expressed GPCR on whole cells (*18, 19*). Selections against live cells remain complicated by the low level of expression of the targeted GPCR in a large background of other cell surface proteins.

The GPCR, Methuselah (Mth), was previously determined to play a role in lifespan in the fruit fly, *Drosophila melanogaster* (*20*). The *mth* mutant exhibits a 35% increase in lifespan and enhanced resistance to various stresses including dietary paraquat, high temperature, and starvation. How Mth actually affects lifespan is unknown, although the *mth* mutant appears defective in synaptic transmission, suggesting a relation between the nervous system with stress resistance and longevity (*21*). As lower expression levels of Mth are associated with its lifespan and stress resistance phenotypes (*20, 21*), ligands for the GPCR, both agonists and antagonists, would potentially be useful as modulators of *Drosophila* aging and as tools for studying GPCR function. The structure of the large, 195-residue extracellular domain was previously determined by crystallography (*22*) and

proposed to contain the natural ligand binding site by analogy to other hormone GPCRs whose isolated ectodomains function in ligand binding (*23-26*).

Here, we have used the Mth ectodomain as a target for *in vitro* selection using mRNA display of a random peptide library. The selected peptides describe a consensus sequence, (R/P)xxWxxR, dubbed the RWR motif. Synthetic peptides bind with high affinity to the ectodomain and recognize full-length Mth expressed in cells. Cell-based GPCR signaling assays were performed using the recently identified Mth agonist, Stunted (*27*), distinguishing several of the selected peptides as strong antagonists. Competition assays suggest that the peptides bind to an interaction "hot spot" (*28*) on the ectodomain, shared by the Stunted binding site. This site appears to be located at an interface between the ectodomain and extracellular loops of Mth, based on a low-resolution crystal structure of a Mth:peptide complex. Additionally, studies of mutant variants of one of the RWR motif peptides has identified a potent Mth agonist that has little homology to Stunted.

Experimental Procedures

Materials

L-[^{35}S]-methionine (1175 Ci/mmol) was purchased from Perkin-Elmer Life Sciences, Inc. (Boston, MA). Other reagents were purchased from Sigma-Aldrich Corp. (St. Louis, MO) or VWR International, Inc. (Boston, MA), unless otherwise specified. Oligos were synthesized at the California Institute of Technology Biopolymer Synthesis and Analysis Facility, except for the 142.1 library template, which was synthesized at the W.M. Keck Facility (Yale University, New Haven, CT). HEK 293 cells expressing Mth-B (HEK-

Mth cells) were generously provided by Prof. Xin-Yun Huang (Cornell University Weill Medical College, New York, NY). DEPC-treated ddH_2O was used for all RNA work.

Expression and immobilization of Methuselah ectodomain

A hexahistidine-tagged Mth ectodomain construct (*22*) was appended with a C-terminal biotinylation tag (*29*) and subcloned into the baculovirus transfer vector pVL1392 (BD Biosciences Pharmingen, San Diego, CA). Mth was purified from supernatants of baculovirus-infected High 5 cells as described previously (*22*). Enzymatic biotinylation with biotin holoenzyme synthetase (BirA) resulted in specific biotinylation at a single lysine residue in the C-terminal tag. Desalting of the biotinylated Mth and immobilization on streptavidin-agarose (Immobilized NeutrAvidin on Agarose, Pierce Biotechnology, Inc., Rockford, IL) produced the target matrix for *in vitro* selection (~1 mg Mth/mL matrix).

mRNA display library preparation

PCR of the 142.1 template (5'-TTA AAT AGC GGA TGC ACG CAG ACC GCC ACT AGT $(SNN)_{27}$ CAT TGT AAT TGT AAA TAG TAA TTG TCC C; N = A, C, G, or T; S = C or G) with the primers 47T7FP (5'-GGA TTC TAA TAC GAC TCA CTA TAG GGA CAA TTA CTA TTT ACA ATT AC) and 21.2 (5'-TTA AAT AGC GGA TGC ACG CAG) produced the initial DNA pool [0.1 μM initial template, 5 total cycles of PCR amplification using Herculase DNA polymerase (Stratagene, La Jolla, CA)]. This library encoded a T7 promoter for transcription, a 5'-UTR sequence, and an ORF for the peptide, M-X_{27}-TSGGLRASAI. After phenol extraction and ethanol precipitation of the DNA, an *in vitro* transcription reaction (80 mM HEPES-KOH at pH 7.5, 2 mM

spermidine, 40 mM DTT, 25 mM $MgCl_2$, 4 mM each of ATP, CTP, GTP, and UTP, and ~6 μg/mL dsDNA template) was treated with RNA*secure* (Ambion, Inc., Austin, TX). T7 RNA polymerase was added and the reaction was incubated at 37 °C for >2 h (*30*). Reactions were quenched with 0.1 volume of 0.5 M EDTA, followed by DNase I treatment (Epicentre, Madison, WI). The mRNA was phenol-extracted with Phase-Lock Gel (Brinkmann Instruments, Inc., Westbury, NY) and isopropanol precipitated prior to gel purification via urea-PAGE. RNA was eluted from gel slices by crushing the acrylamide gel pieces and incubating them in water at 4 °C overnight. Eluted mRNA was filtered and desalted by isopropanol precipitation. Resuspended mRNA was re-treated with DNase I (Invitrogen Corp., Carlsbad, CA), phenol-extracted, and ispropanol-precipitated to ensure complete removal of template DNA.

Cross-linking of a puromycin-psoralen linker to the mRNA was performed essentially as described (*31*). Briefly, mRNA was annealed to oligo 28A.1 (5'-[Ps]-UAG CGG AUG C-dA_{16}-$[S9]_2$-dCdC-[Pu]; where unlabeled bases are 2'-OMe RNA, Ps = psoralen C6, S9 = spacer phosphoramidite 9, and Pu = puromycin-CPG, Glen Research Corp., Sterling, VA) by incubating the mixture (~12.4 μM mRNA, 17.75 μM 28A.1, 12.5 mM HEPES-KOH at pH 7.5, and 250 mM NaCl) at 95 °C for 3 min and slow cooling to 4 °C over 10 min. The reaction was then irradiated under UV light (UVL-56 365 nm lamp, UVP, Inc., Upland, CA) in an open petri dish for ~45 min. RNA-28A.1 was purified by urea-PAGE as described above. Cross-linking reactions could be irradiated in sealed Eppendorf tubes for ~20 min with comparable yields (data not shown).

In vitro translation with the mRNA-28A.1 library was performed in Red Nova Lysate (Novagen) as per the manufacturer's instructions with optimized conditions (100 mM

KOAc, 0.5 mM MgOAc, 0.4 μM mRNA-28A.1, and ~25 μM overall L-methionine; 10 mL total reaction volume) and ^{35}S-methionine (0.5 mCi/mL final). Following the 30 °C incubation, KOAc and $MgCl_2$ were added to 585 mM and 50 mM (final), respectively, and the reaction was incubated on ice for 15 minutes to facilitate RNA-peptide fusion formation (*32*). RNA-peptide fusions were purified by diluting the reaction mixture ~150-fold into 1× isolation buffer [50 mM HEPES-KOH at pH 7.5, 1 M NaCl, 1 mM EDTA, and 0.05% Tween 20 (Bio-Rad Laboratories, Hercules, CA)] and incubating with oligo-dT cellulose (40 mg/mL of translation, New England Biolabs, Inc., Beverly, MA) at 4 °C for 1 h. Oligo-dT cellulose was pelleted by centrifugation (1500 × g for 1 min) and washed extensively with 0.4× isolation buffer in either glass wool-packed disposable columns (Poly-Prep, Bio-Rad) or in 0.45 μm cellulose acetate centrifuge tube filters (Costar Spin-X, Corning, Inc., Corning, NY). RNA-peptide fusions were eluted with a warmed solution of 1 mM β-mercaptoethanol (65 °C), desalted by isopropanol precipitation using linear acrylamide (Ambion) as a carrier, and reverse-transcribed (Superscript II, Invitrogen) with oligo 21.2. The reverse transcription reaction was supplemented with ~0.05% Tween 20 to ensure that the precipitated RNA-peptide fusions were solubilized. Reverse-transcribed fusions were desalted and exchanged into Mth buffer [50 mM HEPES-KOH at pH 7.5, 150 mM NaCl, 1 mM EDTA, 0.1% (w/v) BSA, 1 μg/mL yeast tRNA (Roche Diagnostics Corp., Indianapolis, IN) and 0.05% Tween 20] using a NAP-25 column (Amersham Biosciences Corp., Piscataway, NJ) prior to the selection step.

In vitro *selection*

RNA:cDNA-peptide fusions were incubated with ~0.1 mL of Mth-NeutrAvidin-agarose at 4 °C for 1 h, then filtered and washed on a Poly-Prep column with 4 ×1 mL Mth buffer followed by 2 × 1 mL Mth buffer without BSA/tRNA. Bound fusions were eluted with 2 × 100 μL of 0.15% SDS at room temperature through a 0.45 μm spin filter. After removal of the SDS using SDS-OUT (Pierce) as per the manufacturer's instructions, fusions were isopropanol-precipitated (50 μg/mL linear acrylamide, 1/40 volume of 3 M NaOAc at pH 5.2, and 1 volume of isopropanol). The reduced salt used for isopropanol precipitation was necessary to prevent inhibition of subsequent PCR, due to the high salt introduced by the SDS-OUT reagent. Precipitated cDNA was PCR-amplified to produce the dsDNA pool for the next round of selection or for cloning and subsequent DNA sequencing (TOPO TA cloning for sequencing kit, Invitrogen).

Further rounds of selection were performed as described for the initial round except that *in vitro* translation reactions were smaller (~0.3 mL), less immobilized Mth was used for the selective step (~20 μL), washes were performed in batch, and in rounds 5 through 8, bound fusions were eluted by competition with non-biotinylated Mth (0.5 mg/mL) in Mth buffer without BSA/tRNA. Additionally, rounds 5 through 8 included a pre-clearing step where the precipitated RNA:cDNA-peptide fusions were passed through multiple columns containing NeutrAvidin-agarose and/or protein G-sepharose (Sigma) to remove peptides with high non-specific binding for the immobilization matrix. The flow-through was then used for selection as described above.

In vitro *binding assays of mRNA display libraries*

To assess the binding activity of mRNA display pools from each round of selection, ^{35}S-methionine-labeled RNA-peptide fusions were prepared and purified as described above. Fusions were treated with RNase (DNase-free, Roche) and mixed with ~10 μL of immobilized Mth in Mth buffer. After rotating at 4 °C for 1 h, the matrix was washed with 3 × 0.6 mL of Mth buffer in a 0.45 μm spin filter and bound 28A.1-puromycin-peptide fusions were quantitated by scintillation counting.

Individual clones were also tested in this format by PCR amplification of specific clones (e.g., R8-01 and R8-04) with oligos 47T7FP and 21.2. Competition studies were performed by introducing various concentrations of unlabeled peptides into the binding buffer during the initial binding step.

Peptide synthesis

Peptides were synthesized on a 432A Synergy peptide synthesizer (Applied Biosystems, Foster City, CA) using standard Fmoc chemistry. Synthesized peptides were cleaved and deprotected from the resin by agitation in TFA/1,2-ethanediol/thioanisole (90:5:5) for 2 h at room temperature. After desalting by precipitation in methyltertbutyl ether, crude peptides were purified by reversed-phase HPLC (C18, 250 × 10 mm, Grace Vydac, Hesperia, CA) to >95% purity on an aqueous acetonitrile/0.1% (v/v) TFA gradient. Peptide masses were confirmed by MALDI-TOF mass spectrometry and concentrations were determined by absorbance at 280 nm using a calculated extinction coefficient (http://paris.chem.yale.edu/extinct.html).

Several peptides were synthesized with an N-terminal spacer (ethylene glycol, Bachem California, Inc., Torrance, CA) for conjugation to various functional groups (e.g., biotin, fluorescein, or rhodamine). Prior to deprotection of the peptide and cleavage from the resin, the free N-terminal amine could be coupled to NHS-conjugated compounds (Pierce). Briefly, the peptide resin was incubated with agitation at room temperature for 2 to 4 hours in DMF containing 2- to 5-fold molar excess of the NHS-conjugate. Reactions were quenched with 0.5 M ethanolamine and the resin was washed thoroughly with DMF, DMSO, followed by methanol through a Poly-Prep column on a vacuum manifold. The resin was dried on vacuum before deprotecting and purifying the peptide as described above.

Peptide truncation and mutagenesis series were synthesized with C-terminal glycines by JPT Peptide Technologies GmbH (MicroScale Peptide Sets, Berlin, Germany). Crude, dried peptides were provided in 96-well plates at approximately 50 nmol of full-length peptide per well. Peptides were reconstituted in 20 μL of DMSO (~2.5 mM stock concentration) prior to their use in cell signaling assays.

Kinetics determination by surface plasmon resonance (SPR)

SPR measurements were performed at 25 °C on a BIAcore 2000 instrument (Biacore, Inc., Piscataway, NJ) equipped with research-grade SA (streptavidin) sensor chips. Biotinylated Mth was immobilized to a surface density of 450 to 700 response units (RU). HBS-EP [10 mM HEPES at pH 7.4, 150 mM NaCl, 3 mM EDTA, and 0.005% polysorbate 20 (Tween 20), Biacore] was used as the running buffer for all experiments. To collect kinetics data, a concentration series of each peptide was injected for at least 60

s at a flow rate of >45 μL/min. Peptides were allowed to freely dissociate to background between injections (~5 min). Buffer blank injections were used for double referencing with a negative control surface (*33*). Raw data was processed with Scrubber and globally fit with CLAMP using a 1:1 bimolecular interaction model (*34*). K_D values were calculated (k_d/k_a) from the determined rate constants.

Spectrofluorometric analysis of Mth:peptide complexes

Measurements of intrinsic tryptophan and tyrosine fluorescence spectra were performed on a spectrofluorophotometer (RF-5301PC, Shimadzu Scientific Instruments, Columbia, MD) at excitation wavelengths of 280 or 295 nm (slit width set at 3 nm). Spectra were taken at room temperature from 260 to 450 nm at 0.2 nm intervals (medium speed, 3 or 5 nm slit widths for R8-12 or R8-04 peptides, respectively). Complexes were formed by mixing equimolar concentrations of peptide and Mth ectodomain in buffer (10 mM KH_2PO_4 at pH 7.2 and 150 mM NaCl) for 5 min before taking fluorescence readings in a stirred cell. For R8-04, 3 μM peptide and wild-type Mth ectodomain were used. The mutant ectodomain, Mth W120S, was used for complexes with R8-12 (both at 6.25 μM concentrations) because the peptide contains a single Trp residue. For the fluorescence titration study, 300 nM of R8-12 peptide was used and aliquots of Mth W120S were directly added to a stirring cell (excitation and emission wavelengths were set at 295 and 345 nm, with slit widths at 5 and 10 nm, respectively).

Crystallography – data collection, structure solution, and refinement

Purified His_6-tagged Mth ectodomain (15 mg/mL) was mixed with 1.5-fold molar excess R8-01 15-mer peptide in 10 mM Tris at pH 8.0. Crystals of the Mth:R8-01 complex were

grown by hanging drop, in which the protein mixture was mixed 1:1 with well solution [0.1 M HEPES-KOH at pH 7.5, 1.7 M ammonium sulfate, and 2% (w/v) PEG 400]. The resulting 2 μL drop was suspended over 0.8 mL of well solution. Crystals were grown for several months at room temperature and formed long rods with maximum dimensions of 200 μm × 50 μm × 50 μm.

Crystals were transferred to a cryoprotectant solution [(0.1 M HEPES-KOH at pH 7.5, 1.8 M ammonium sulfate, 2% PEG 400, and 20% (v/v) glycerol] prior to flash cooling. Data were collected at −150 °C at the Advanced Light Source beamline 9.2.2 with λ = 1.0781 Å. Data were processed and scaled with DENZO and SCALEPACK (*35*). The diffraction was strongly anisotropic, extending to ~2.5 Å along the 4-fold axis but only to ~3.8 Å perpendicular to the 4-fold with strong streaking in these directions. The crystals were initially indexed in space group $P4_2$, with a = 94.25 Å and c = 173.84 Å. R_{merge} from 20–3.50 Å (3.62–3.50 Å) was 15.5% (37.0%).

The structure was determined by molecular replacement using AMoRe (*36*) from version 5 of the CCP4 suite (*37*) with the 2.3 Å structure of the Mth ectodomain (PDB code 1FJR) as a search model. Examination of the native Patterson map revealed three very strong non-origin peaks implying translational non-crystallographic symmetry (NCS). A translational NCS vector was used during the translation function search. Two molecules were placed in the asymmetric unit, which explained two of the three peaks in the native Patterson. Addition of a third molecule, necessary to give the third native Patterson peak, always resulted in steric clashes. The data was eventually explained by a certain type of stacking disorder in the crystals, which was consistent with the observed symmetry of the Mth packing. This disorder is the likely cause of the strong anisotropy

of the data and of the streaking of the diffraction spots. We modeled the disorder with one Mth molecule with unit occupancy and two with half occupancy. Maps were calculated with solvent flattening, histogram matching, and NCS averaging using the program DM in the CCP4 suite (*37*). Anisotropy and bulk solvent corrections were applied and the model was refined with NCS constraints using grouped temperature (*B*) factors using the program CNS (*38*). The peptide has been left unmodeled. The current model has R_{cryst} = 37.5% and R_{free} = 40.8%.

Fluorescence labeling of cells expressing Methuselah

Chinese hamster ovary (CHO) cells were transiently transfected with a Mth-GFP fusion construct and grown in alpha-MEM with 5% fetal bovine serum (FBS). Cells were detached by trypsination and washed with P4F (1× PBS with 4% FBS). Cells were then incubated with 150 nM rhodamine-R8-12 peptide in P4F for 1 hour at 4 °C, washed extensively with P4F, and either mounted on glass slides for fluorescence microscopy or sorted by FACS (BD FACSCalibur System, BD Biosciences Immunocytometry Systems, San Jose, CA).

Cell-based GPCR signaling assay

HEK 293 cells expressing Mth-B were plated in clear-bottom 96-well plates (Corning) at ~25% confluency using Matrigel (BD Biosciences). Supernatant was removed by careful aspiration and each well was washed with 200 μL of buffer F [20 mM HEPES-KOH at pH 7.5, 0.1% BSA, and 2.5 mM probenicid (dissolved first in 1/100 volume of 1 M NaOH) in Hanks' balanced salt solution without phenol red (HBSS, Invitrogen)]. Fluo-4 (4 μM, dissolved first in 20 μL of 1:1 DMSO:10% Pluronic F-127, Molecular Probes,

Eugene, OR) in buffer F with 1% BSA was added to each well (100 μL) and the plate was incubated at room temperature for 45 min, followed by incubation at 37 °C for 15 min. Wells were washed with 3 × 200 μL of buffer F while the plate was on ice. For agonist assays, 100 μL of buffer F was added to each well and the plate was incubated at 37 °C for 15 min prior to starting the experiment. Fluorescence measurements and automated sample delivery were performed in Flexstation mode on a robotic plate reader (Flexstation, Molecular Devices, Sunnyvale, CA). Agonist peptides in reagent buffer (20 mM HEPES-KOH at pH 7.5 and 5% DMSO in HBSS) were added (50 μL) after an initial baseline reading (30 to 45 s). Continuous readings were made for ~5 min (7 reads/well, 2 s intervals, 494 nm excitation wavelength, 520 nm emission, and 515 nm cutoff filter). For antagonist assays, 80 μL of buffer F was added to each well prior to the 15 min 37 °C incubation. Potential antagonists were added (20 μL) after the baseline readings followed by addition of the agonist peptide (50 μL). Data analysis and background subtraction were performed with Softmax Pro 4.7.1 (Molecular Devices). Sigmoidal fits were calculated using Origin 6.0 Professional (OriginLab Corp., Northampton, MA).

Results

In vitro *selection of ligands for the Methuselah ectodomain*

The mature, N-terminal ectodomain of Mth is a stably folded, glycosylated protein of 195 residues (*22*). By analogy to other GPCRs with large, extracellular N-terminal domains that maintain recognition of their cognate ligands independently of their transmembrane cores (*23-26*), we targeted the Mth ectodomain for *in vitro* selection to isolate putative modulators of Mth signaling. A random, 27-mer peptide library was constructed for

selection using mRNA display. Based on quantitation of the purified, ^{35}S-labeled RNA-peptide fusions and the estimated L-methionine concentration, the complexity of the starting library was approximately 1.5×10^{13}. Because the hexahistidine tag is a weak epitope for peptide selections (see Appendix A), a specifically biotinylated construct of the Mth ectodomain was expressed and purified using a C-terminal peptide substrate sequence recognized by BirA (*29*). Four rounds of selection were initially performed and, although binding to the Mth ectodomain was above background levels, a high degree of non-specific binding to the matrix was observed (Figure 1A). Four subsequent rounds of selection were performed which included preclearing steps on matrix without target and specific elution with free, non-biotinylated Mth. The final 8th round pool exhibited negligible non-specific binding and high activity for Mth.

DNA sequencing of individual clones from the final selection round (Table I) revealed a highly conserved consensus motif, (R/P)xxWxxR, dubbed the RWR motif (Figure 1B). Interestingly, 6 out of 7 sequences in the 5th round pool (Supplemental Table I) encoded at least WxxR. Amino acid analysis of the selected peptides, however, revealed a shift toward more polar residues in the 8th round pool. This suggests that the multiple rounds of preclearing and specific elution succeeded in retaining the binding motif (and hence, affinity for the Mth ectodomain) while reducing non-specific interactions.

Analysis of the amino acid types at each position in the aligned peptides revealed a degree of covariation in the RWR motif depending on whether the first residue of the motif is Arg or Pro (Figure 1C and D). Arg is generally followed by two non-polar residues, while Pro is followed by charged or polar amino acids. This trend is most

evident in the 8th round sequences, but is also observed in RWR motif peptides in the previous rounds. Residues 6 and 7 in the WxxR consensus are generally non-polar, while residue 9, immediately C-terminal to the RWR motif, is almost always polar, especially favoring Ser or Thr. There also seems to be a weak preference for Arg an indiscriminant number of residues C-terminal to the RWR motif. Phe-Arg, Ala-Arg, and especially Leu-Arg were often observed 5 to 7 residues downstream of the RWR motif (Figure 1B and Supplemental Table I).

Binding kinetics determined by surface plasmon resonance

Several selected peptides were synthesized and purified for binding analysis by SPR (Table II). Peptides were designed to include the RWR motif and an additional number of flanking residues. *In vitro* binding studies with C-terminal truncations of an outlier peptide R8-04 (a recovered peptide that lacked an RWR motif), suggested that the full-length peptide was important for high affinity binding. Hence, R8-04 was synthesized through the first 3 residues encoded by the 3' constant region. Mth-binding peptides containing the RWR motif demonstrated high affinity (K_D <30 nM) while R8-04 exhibited a K_D of 330 nM (Table III). Binding was not observed at concentrations of up to 1 μM for the W7A and R10A mutants of R8-14, demonstrating the importance of these conserved residues for Mth-binding. Weak binding was observed with 1 μM of a scrambled R8-01 peptide (R8-01 SCR). Higher concentrations, however, were not tested by SPR.

Hot spot for Methuselah interaction

Sequential binding of peptides R8-01, R8-04, and R8-12 was also analyzed by SPR and strongly suggested that the selected peptides share the same binding site (data not shown). This was demonstrated more clearly in competition binding studies (Figure 2A). Synthetic, unlabeled peptide R8-01 competed for binding to immobilized Mth ectodomain with both radiolabeled, full-length R8-01 and R8-04. The weak affinity of R8-01 SCR was confirmed as it also competed for binding to Mth. Interestingly, a synthetic variant of the recently isolated peptide agonist for Mth, Stunted (*27*), also competed for binding, demonstrating that the natural ligand binding site is an interaction "hot spot" (*28*) and at least partially reconstituted by the Mth ectodomain.

The Mth ectodomain contains a single solvent-exposed Trp residue in a shallow groove that was proposed to be a potential binding site for the natural ligand (*22*). Mth W120S, where the Trp was mutated to a Ser, was constructed to assay the effect of this mutation on binding for the R8-12 peptide, which contains a single Trp at position 5. Mth W120S expresses similarly to the wild-type ectodomain and CD spectra of the two proteins were nearly identical, suggesting that the mutant folds stably (data not shown). Excitation at 295 nm, which is specific for tryptophan residues, revealed a significant fluorescence enhancement of Trp5 in the R8-12 peptide upon binding to Mth W120S (Figure 2B). The maximum fluorescence wavelength (λ_{max}) of 351 nm for R8-12 is indicative of denatured proteins, suggesting that the peptide is unstructured in solution. The blue-shift of λ_{max} to 343 nm, as well as the increase in fluorescence, suggests that R8-12 Trp5 is at least partially buried upon binding to Mth W120S and protected from solvent quenching. The fluorescence contributions from Tyr residues (λ_{max} = ~302 nm)

could be observed by excitation at 280 nm, which revealed a negligible change in signal upon peptide binding (data not shown). The K_D of R8-12 binding to Mth W120S was also determined by fluorescence titration and calculated to be 15 nM, which compares well with results from the SPR studies (Figure 2B, inset).

Fluorescence spectra were also measured for wild-type Mth ectodomain in complex with peptide R8-04, which does not contain a Trp residue. The fluorescence spectra were nearly identical, however, between Mth and the Mth:R8-04 complex (Figure 2C). The concentration of each component (3 μM) was ~10-fold greater than the K_D determined by SPR, suggesting that the lack of a fluorescence change was probably not due to inadequate complex formation. If the R8-04 peptide were interacting near Trp120, a much greater effect on Trp fluorescence would be expected upon binding. The resulting spectra, along with the R8-12 data, suggest that the Mth interdomain groove containing Trp120 is not the shared binding site for the selected peptides and the N-Stunted agonist.

To determine the precise location of the peptide binding site, the structure of the Mth ectodomain in complex with an RWR motif peptide was determined by crystallography. Although the resulting data was low-resolution (3.5–4 Å), electron density which putatively corresponds to the R8-01 15-mer peptide places the binding site near the C-terminus of the ectodomain. This suggests that the peptides bind at or near an interface between the Mth ectodomain and extracellular loops (Figure 3). Interestingly, the 2nd extracellular loop (EL2) between the 4th and 5th transmembrane helices contains a WxxR peptide sequence (a partial RWR motif) which may interact in the same region as the selected peptides.

Fluorescent peptide probes recognize the full-length GPCR

While the peptides bound with high affinity to the Mth ectodomain, it was important to determine whether they would still recognize the full-length GPCR. A full-length Mth-GFP fusion construct was expressed in a CHO cell line, stained with a rhodamine-tagged R8-12 peptide, and examined by fluorescence microscopy, revealing strong labeling of cells expressing the Mth-GFP fusion protein (Figure 4A). Staining was not observed on cells incubated with a rhodamine-labeled, scrambled version of R8-12 (data not shown). The CHO/Mth-GFP cells were also amenable to sorting by FACS, demonstrating a linear correlation between Mth-GFP expression and the degree of rhodamine staining (Figure 4B). These rhodamine-peptide probes were functional for labeling Mth-GFP over-expressed in *Drosophila* larvae and adults, but the use of wild-type and control flies did not result in any specific, punctate staining of endogenous Mth (data not shown). This may be due to a low level of endogenous Mth expression or cross-reactivity of our probes to Mth homologs.

Selected peptides act as antagonists for Methuselah signaling

Recently, Stunted, the endogenous agonist for Mth, was isolated from adult *Drosophila* extracts using a cell-based, fluorescence reporter system (*27*). HEK-Mth cells were loaded with a fluorescent calcium indicator and washed prior to the assay. Addition of a Mth agonist induced calcium flow into the cell and a subsequent increase in fluorescence. Synthetic 30-mer peptides corresponding to the N- and C-terminal halves of the ~60-mer Stunted were also tested, isolating the agonist activity to the N-terminus (N-Stunted). By pre-incubating cells with selected peptides prior to the addition of the N-Stunted agonist,

any antagonist activity from the peptides could be observed (Figure 5A). R8-12 and R8-14 were strong antagonists of N-Stunted-induced Mth signaling, with IC_{50} values of 70 and 170 nM, respectively (Figure 5B). R8-01 also acted as an antagonist, though an IC_{50} was not determined. The W7A and R10A mutants of R8-14 did not exhibit any antagonist activity. In all cases, signaling was not observed on non-transfected, control HEK 293 cells (data not shown).

Biochemical characterization of Stunted and a novel peptide agonist

Surprisingly, strong calcium signaling was observed upon addition of the R8-01 scrambled peptide to HEK-Mth cells (Figure 6A). The activity was specific to cells expressing Mth, in comparison with a non-transfected control cell line (data not shown), and suggested that R8-01 SCR is a specific Mth agonist. The R8-01 SCR peptide shares few residues in common with N-Stunted and appeared to be a more potent activator of Mth (EC_{50} of 2.5 μM, compared with 11 μM for N-Stunted, Figure 6B). The inhibition of R8-01 SCR-mediated signaling by the selected peptides, R8-12 and R8-14, provides further evidence that the scrambled peptide is indeed a specific agonist for Mth (Figure 6C).

A series of 15-mer peptides for N-Stunted and 12-mers for R8-01 SCR were synthesized to determine the minimal peptide that exhibited agonist activity. Crude peptides were tested directly in the cell-based assay for Mth activation. For N-Stunted, the region of activity was localized to the N-terminus (Figure 7A). As the first 3 peptides in the series were functional, this suggests that the minimal peptide sequence required for maximal activity is AWRAAGITYIQYS. The C-terminal peptides of N-Stunted also

exhibited some activity above background, although it is inconclusive whether a second local region of agonist activity exists, or if this is caused by something non-specific. For R8-01 SCR, the minimal peptide with high activity appears to be LQAPRRSVMRW.

Discussion

High affinity peptide ligands that act as antagonists to the recently isolated, endogenous Mth agonist, Stunted, were isolated by *in vitro* selection using a naïve, random 27-mer mRNA display library targeting the Mth ectodomain. Most of the unique sequences encoded a consensus, the RWR motif (R/P)xxWxxR. However, it appears that all the selected peptides, including R8-04 which was an "outlier" sequence lacking the RWR motif, bind to the same site on the Mth ectodomain, a putative "hot spot" for interaction.

Curiously, the final selection pool was dominated by the outlier peptide, R8-04, which also exhibited the weakest binding. The competitive elution with free, non-biotinylated Mth ectodomain in the last few rounds of selection most likely enriched the pool for the weakest binding peptides. Those peptides with the fastest off rates would be competed first. While we attempted to optimize the incubation time for the elution, our main goal was to eliminate the non-specific binding peptides. A selection against the Mth ectodomain with a "doped" peptide library, encoding the RWR motif, may be useful in isolating new sequences with even higher affinities. It is interesting that although the earlier 5^{th} round pool demonstrated moderate non-specific binding to various immobilization matrices, the clones had already encoded the RWR motif. More stringent selection conditions in the later rounds enriched RWR motif peptides with fewer hydrophobic residues and low non-specific binding.

The RWR motif is a very strong consensus, with other amino acids generally conserved. The C-terminal preference for Arg and especially certain Arg pairs were found a variable number of residues away from the RWR motif. Hence, the region immediately following the motif may not be highly structured. The placement of the RWR motif in the random region of the selected peptides appears random. Hence, the preference for a Leu-Arg sequence C-terminal to the RWR motif may not be very strong, as the constant region encoded a Leu-Arg–containing sequence.

In vitro studies suggested that R8-04 binds significantly better with the C-terminal constant region than without (data not shown). Because *in vitro* translation can start at alternate methionine codons, N-terminal truncations of R8-04 were also observed. Interestingly, N-terminal truncations were non-binding. Hence, the full-length, 38-mer R8-04 peptide (which includes the entire C-terminal constant region) may bind significantly better than the 31-mer used in our experiments and may do so in some folded structure that utilizes both termini.

The random scrambling of the R8-01 peptide was performed to ensure that the RWR motif was not retained. However, while the RxxWxxR motif was eliminated, the new peptide did encode a PxxSxxR sequence which may still have minimal affinity. Further study of the R8-01 scrambled agonist, as well as mutational studies of the other peptides, may reveal the critical residues in converting an antagonist (R8-01) to an agonist (R8-01 SCR). Not only was the R8-01 SCR a more potent agonist than Stunted, but the Stunted peptide also exhibited delayed activation of the receptor (Figure 6A). The isolation of a novel, potent agonist for Mth with little homology to Stunted suggests that other, natural endogenous Mth ligands may exist that have yet to be identified. The minimal, active

region of N-Stunted identified in our studies corresponds well to the most conserved region of Stunted homologs, the epsilon subunit of the eukaryotic F1-ATPase (*39*), further suggesting that N-Stunted is indeed one of the natural endogenous ligands for Mth.

The localization of the peptide binding site to a putative interface between the Mth ectodomain and extracellular loops suggests that the WxxR on EL2 (a partial RWR motif) may form similar interactions with the ectodomain as our peptides. An interaction between a synthetic EL2 peptide (at concentrations up to 150 μM) and the Mth ectodomain was not observed in *in vitro* competition studies (Table II and data not shown). This may not preclude an *in vivo* interaction, however, as the affinity between EL2 and the ectodomain may be extremely low, but compensated for in the full-length receptor where the EL2 sequence and the ectodomain are co-localized. Additionally, a high affinity, optimized interaction may be undesirable for natural signaling.

We have successfully isolated novel peptide ligands for a GPCR using mRNA display selection libraries targeting the extracellular domain of Mth. The application of these peptides toward the synthetic extension of *Drosophila* lifespan is currently being tested. Whether mRNA display can be generally used against full-length GPCR targets has yet to be determined. Targeting GPCRs expressed in cells remains an unattractive option due to the large background of cell surface proteins. The recent success in assembling paramagnetic proteoliposomes containing pure GPCRs is a favorable alternative for a selection target (*40*). The development of suitable expression and display platforms for transmembrane proteins will greatly facilitate the selection of peptide modulators of GPCR signaling.

Acknowledgments

We thank Dr. Anthony M. Giannetti for technical expertise on the Biacore, Prof. David G. Myszka (University of Utah) for the SPR analysis software, Scrubber and CLAMP, Prof. Melvin I. Simon for use of the Flexstation automated fluorescence plate reader, and Prof. Theodore Brummel (Sam Houston State University, TX) and Dr. David Walker for helpful discussions. We also thank Terry T. Takahashi for comments on the manuscript. We are greatly indebted to Dr. Svetlana Cvejic and Prof. Xin-Yun Huang (Cornell University Weill Medical College, NY) for providing the HEK-Mth cell lines and details on their protocols. We are especially grateful to Dr. Peter M. Snow (deceased 2004) for preparative expertise on protein purification.

This work was supported by grants from the NIH (RO160416) and the Beckman Foundation to R. W. R. W. W. J. was supported in part by a DOD National Defense Science and Engineering Graduate Fellowship and a Scholarship for Research in the Biology of Aging, sponsored by the Glenn Foundation for Medical Research and the American Federation for Aging Research. A. P. W., Jr., was supported by a Career Award in the Biomedical Sciences from the Burroughs Wellcome Fund. R. W. R. is an Alfred P. Sloan Foundation Research Fellow.

References

1. Strader, C. D., Fong, T. M., Tota, M. R., Underwood, D., and Dixon, R. A. F. (1994) Structure and function of G protein-coupled receptors, *Annu. Rev. Biochem. 63*, 101-132.

2. Drews, J. (2000) Drug discovery: a historical perspective, *Science 287*, 1960-1964.

3. Howard, A. D., McAllister, G., Feighner, S. D., Liu, Q., Nargund, R. P., Van der Ploeg, L. H. T., and Patchett, A. A. (2001) Orphan G-protein-coupled receptors and natural ligand discovery, *Trends Pharmacol. Sci. 22*, 132-140.

4. Milligan, G. (2002) Strategies to identify ligands for orphan G-protein-coupled receptors, *Biochem. Soc. Trans. 30*, 789-793.

5. Szekeres, P. G. (2002) Functional assays for identifying ligands at orphan G protein-coupled receptors, *Receptor. Channel. 8*, 297-308.

6. Dower, W. J., and Mattheakis, L. C. (2002) *In vitro* selection as a powerful tool for the applied evolution of proteins and peptides, *Curr. Opin. Chem. Biol. 6*, 390-398.

7. Lin, H., and Cornish, V. W. (2002) Screening and selection methods for large-scale analysis of protein function, *Angew. Chem. Int. Edit. 41*, 4402-4425.

8. Ja, W. W., and Roberts, R. W. (2004) *In vitro* selection of state-specific peptide modulators of G protein signaling using mRNA display, *Biochemistry 43*, 9265-9275.

9. Cain, S. A., Williams, D. M., Harris, V., and Monk, P. N. (2001) Selection of novel ligands from a whole-molecule randomly mutated C5a library, *Protein Eng. 14*, 189-193.

10. Heller, T., Hennecke, M., Baumann, U., Gessner, J. E., zu Vilsendorf, A. M., Baensch, M., Boulay, F., Kola, A., Klos, A., Bautsch, W., and Köhl, J. (1999) Selection of a C5a receptor antagonist from phage libraries attenuating the inflammatory response in immune complex disease and ischemia/reperfusion injury, *J. Immunol. 163*, 985-994.

11. Szardenings, M., Törnroth, S., Mutulis, F., Muceniece, R., Keinänen, K., Kuusinen, A., and Wikberg, J. E. (1997) Phage display selection on whole cells yields a peptide specific for melanocortin receptor 1, *J. Biol. Chem. 272*, 27943-27948.

12. Rousch, M., Lutgerink, J. T., Coote, J., de Bruïne, A., Arends, J.-W., and Hoogenboom, H. R. (1998) Somatostatin displayed on filamentous phage as a receptor-specific agonist, *Br. J. Pharmacol. 125*, 5-16.

13. Doorbar, J., and Winter, G. (1994) Isolation of a peptide antagonist to the thrombin receptor using phage display, *J. Mol. Biol. 244*, 361-369.

14. Goodson, R. J., Doyle, M. V., Kaufman, S. E., and Rosenberg, S. (1994) High-affinity urokinase receptor antagonists identified with bacteriophage peptide display, *Proc. Natl. Acad. Sci. U.S.A. 91*, 7129-7133.

15. Houimel, M., Loetscher, P., Baggiolini, M., and Mazzucchelli, L. (2001) Functional inhibition of CCR3-dependent responses by peptides derived from phage libraries, *Eur. J. Immunol. 31*, 3535-3545.

16. Moulard, M., Phogat, S. K., Shu, Y., Labrijn, A. F., Xiao, X., Binley, J. M., Zhang, M.-Y., Sidorov, I. A., Broder, C. C., Robinson, J., Parren, P. W. H. I., Burton, D. R., and Dimitrov, D. S. (2002) Broadly cross-reactive HIV-1-neutralizing human monoclonal Fab selected for binding to gp120-CD4-CCR5 complexes, *Proc. Natl. Acad. Sci. U.S.A. 99*, 6913-6818.

17. Osbourn, J. K., Earnshaw, J. C., Johnson, K. S., Parmentier, M., Timmermans, V., and McCafferty, J. (1998) Directed selection of MIP-1α neutralizing CCR5 antibodies from a phage display human antibody library, *Nat. Biotechnol. 16*, 778-781.

18. Hoogenboom, H. R., Lutgerink, J. T., Pelsers, M. M. A. L., Rousch, M. J. M. M., Coote, J., van Neer, N., de Bruïne, A., van Nieuwenhoven, F. A., Glatz, J. F. C., and Arends, J.-W. (1999) Selection-dominant and nonaccessible epitopes on cell-surface receptors revealed by cell-panning with a large phage antibody library, *Eur. J. Biochem. 260*, 774-784.

19. Sui, J., Bai, J., St Clair Tallarico, A., Xu, C., and Marasco, W. A. (2003) Identification of CD4 and transferrin receptor antibodies by CXCR4 antibody-guided Pathfinder selection, *Eur. J. Biochem. 270*, 4497-4506.

20. Lin, Y.-J., Seroude, L., and Benzer, S. (1998) Extended life-span and stress resistance in the *Drosophila* mutant *methuselah*, *Science 282*, 943-946.

21. Song, W., Ranjan, R., Dawson-Scully, K., Bronk, P., Marin, L., Seroude, L., Lin, Y.-J., Nie, Z., Atwood, H. L., Benzer, S., and Zinsmaier, K. E. (2002) Presynaptic regulation of neurotransmission in *Drosophila* by the G protein-coupled receptor Methuselah, *Neuron 36*, 105-119.

22. West, A. P., Jr., Llamas, L. L., Snow, P. M., Benzer, S., and Bjorkman, P. J. (2001) Crystal structure of the ectodomain of Methuselah, a *Drosophila* G protein-coupled receptor associated with extended lifespan, *Proc. Natl. Acad. Sci. U.S.A. 98*, 3744-3749.

23. Cao, Y.-J., Gimpl, G., and Fahrenholz, F. (1995) The amino-terminal fragment of the adenylate cyclase activating polypeptide (PACAP) receptor functions as a high affinity PACAP binding domain, *Biochem. Biophys. Res. Commun. 212*, 673-680.

24. Chow, B. K. (1997) Functional antagonism of the human secretin receptor by a recombinant protein encoding the N-terminal ectodomain of the receptor, *Recept. Signal Transduct. 7*, 143-150.

25. Grauschopf, U., Lilie, H., Honold, K., Wozny, M., Reusch, D., Esswein, A., Schäfer, W., Rücknagel, K. P., and Rudolph, R. (2000) The N-terminal fragment of human parathyroid hormone receptor 1 constitutes a hormone binding domain and reveals a distinct disulfide pattern, *Biochemistry 39*, 8878-8887.

26. Wilmen, A., Göke, B., and Göke, R. (1996) The isolated N-terminal extracellular domain of the glucagon-like peptide-1 (GLP)-1 receptor has intrinsic binding activity, *FEBS Lett. 398*, 43-47.

27. Cvejic, S., Zhu, Z., Felice, S. J., Berman, Y., and Huang, X.-Y. (2004) The endogenous ligand Stunted of the GPCR Methuselah extends lifespan in *Drosophila*, *Nat. Cell Biol. 6*, 540-546.

28. Clackson, T., and Wells, J. A. (1995) A hot spot of binding energy in a hormone-receptor interface, *Science 267*, 383-386.

29. Schatz, P. J. (1993) Use of peptide libraries to map the substrate specificity of a peptide-modifying enzyme: a 13 residue consensus peptide specifies biotinylation in *Escherichia coli*, *Bio-Technol. 11*, 1138-1143.

30. Milligan, J. F., and Uhlenbeck, O. C. (1989) Synthesis of small RNAs using T7 RNA polymerase, *Methods Enzymol. 180*, 51-62.

31. Kurz, M., Gu, K., and Lohse, P. A. (2000) Psoralen photo-crosslinked mRNA-puromycin conjugates: a novel template for the rapid and facile preparation of mRNA-protein fusions, *Nucleic Acids Res. 28*, e83.

32. Liu, R., Barrick, J. E., Szostak, J. W., and Roberts, R. W. (2000) Optimized synthesis of RNA-protein fusions for *in vitro* protein selection, *Methods Enzymol. 318*, 268-293.

33. Myszka, D. G. (2000) Kinetic, equilibrium, and thermodynamic analysis of macromolecular interactions with BIACORE, *Methods Enzymol. 323*, 325-340.

34. Myszka, D. G., and Morton, T. A. (1998) CLAMP (c): A biosensor kinetic data analysis program, *Trends in Biochemical Sciences 23*, 149-150.

35. Otwinowski, Z., and Minor, W. (1997) Processing of x-ray diffraction data collected in oscillation mode, *Methods Enzymol. 276*, 307-326.

36. Navaza, J. (1994) AMoRe: an automated package for molecular replacement, *Acta Crystallogr. A 50*, 157-163.

37. Collaborative Computational Project, N. (1994) The CCP4 suite: programs for protein crystallography, *Acta Crystallogr. D 50*, 760-763.

38. Brünger, A. T., Adams, P. D., Clore, G. M., DeLano, W. L., Gros, P., Grosse-Kunstleve, R. W., Jiang, J.-S., Kuszewski, J., Nilges, M., Pannu, N. S., Read, R.

J., Rice, L. M., Simonson, T., and Warren, G. L. (1998) Crystallography & NMR system: A new software suite for macromolecular structure determination, *Acta Crystallogr. D 54*, 905-921.

39. Tu, Q., Yu, L., Zhang, P., Zhang, M., Zhang, H., Jiang, J., Chen, C., and Zhao, S. (2000) Cloning, characterization and mapping of the human *ATP5E* gene, identification of pseudogene *ATP5EP1*, and definition of the ATP5E motif, *Biochem. J. 347*, 17-21.

40. Mirzabekov, T., Kontos, H., Farzan, M., Marasco, W., and Sodroski, J. (2000) Paramagnetic proteoliposomes containing a pure, native, and oriented seven-transmembrane segment protein, CCR5, *Nat. Biotechnol. 18*, 649-654.

41. Schneider, T. D., and Stephens, R. M. (1990) Sequence logos: a new way to display consensus sequences, *Nucleic Acids Res. 18*, 6097-6100.

42. Crooks, G. E., Hon, G., Chandonia, J. M., and Brenner, S. E. (2004) WebLogo: a sequence logo generator, *Genome Res. 14*, 1188-1190.

43. Palczewski, K., Kumasaka, T., Hori, T., Behnke, C. A., Motoshima, H., Fox, B. A., Le Trong, I., Teller, D. C., Okada, T., Stenkamp, R. E., Yamamoto, M., and Miyano, M. (2000) Crystal structure of rhodopsin: A G protein-coupled receptor, *Science 289*, 739-745.

Tables

Table I. Peptide sequences from the 8th round of selection.[a]

Peptide	Sequence		Frequency
R8-08b	SSLSPPWPASWSPSRPSAPRAAPSTPT	*	2/20
R8-04	VRIGYTSKPGGMNPGNSYTMSIIRMLI		7/20
R8-07b	STAGSRARSTS**W**GT**R**SPWTWPTPARTG	*	
R8-01	NVSWGSF**P**SS**W**LQ**R**YYLAKRREADVTL		4/20
R8-07	LKY**P**DT**W**LA**R**SLSVFYLRKSARQGKSV		
R8-13	ELGQFQRLSL**P**YQ**W**YL**R**TISYVSLRTA		
R8-03	GDDMYRIREFLANY**R**PI**W**VM**R**SNLAQL		
R8-12	**R**LV**W**IV**R**SRHFGPRLRMALLGSDRKMW		
R8-14	AP**R**AV**W**IQ**R**AIQAMFRLASRQESKAFN		
R8-09b	**R**YV**W**YL**R**TKHRRSLRLRSACARGSSA	*	

[a] The frequency (out of 20) is shown for peptides that appeared more than once from DNA sequencing of individual clones. The methionine start codon and C-terminal constant region (TSGGLRASAI), which was frame-shifted or mutated in marked sequences (*), are not shown.

Table II. Synthesized peptide sequences.

Peptide	Sequence
R8-01	MNVSWGSFPSSWLQRYYLAKRR
R8-01 SCR	SWSLQAPRRSVMRWYGFYLNKS
R8-01 15-mer	FPSSWLQRYYLAKRR
R8-04	MVRIGYTSKPGGMNPGNSYTMSIIRMLITSG
R8-12	MRLVWIVRSRHFGPRLRMA
R8-12 SCR	MLRARRHGVWSPLRFRIMV
R8-14	MAPRAVWIQRAIQAMFRLA
R8-14 W7A [a]	MAPRAVAIQRAIQAMFRLAGY
R8-14 R10A	MAPRAVWIQAAIQAMFRLA
N-Stunted	MTAWRAAGITYIQYSNIAARILRESLKTGL
Mth EL2 [b]	DNIVENQDWNPRVGHEGH

[a] The R8-14 W7A mutant was synthesized with a C-terminal Gly-Tyr for quantitation by UV absorbance.

[b] The Mth EL2 sequence is derived from a section of the 2nd extracellular loop of Mth.

Table III. Kinetic parameters for binding of selected peptides with Mth, as determined by SPR.[a]

Peptide	$\mathbf{k_a}$	$\mathbf{k_d}$	$\mathbf{K_D}$[b]	$\boldsymbol{\chi^2}$
	$M^{-1}s^{-1}$ ($\times 10^5$)	s^{-1} ($\times 10^{-2}$)	*nM*	
R8-01	6.3	1.9	31	1.5
R8-01 15-mer	9.5	5.4	57	0.46
R8-01 SCR			WB	
R8-12	4.1	0.72	18	1.3
R8-14	7.0	1.2	18	1.7
R8-14 W7A			NB	
R8-14 R10A			NB	
R8-04[c]	6.1	19.9	326	0.46

[a] A sensorgram for one of the SPR experiments with R8-04 is shown in Supplemental Figure 1.
[b] K_D values were calculated (k_d/k_a) from kinetic parameters. Control peptides were non-binding (NB) or weakly binding (WB) at concentrations up to 1 μM.
[c] Peptide sequences are shown in Table II.

Figures

Figure 1. Selection of a 27-mer peptide library against the Mth ectodomain. (A) RNase-treated, ^{35}S-methionine-labeled mRNA displayed peptides from each round of selection were assayed for binding to immobilized Mth (black) or to matrix alone (white). Preclearing and competitive elutions were performed in the 5th through 8th rounds to eliminate non-specific binding peptides. (B) Sequence logo (*41*) representation of RWR motif peptides (13 sequences), indicating the conservation at each amino acid position. Selected peptides containing the RWR motif, (R/P)xxWxxR, were aligned manually and parsed (keeping 1 residue N-terminal and 10 residues C-terminal to the motif). The sequence logo was generated using WebLogo (*42*) at http://weblogo.berkeley.edu. Residues are colored according to amino acid type, as indicated. The same color-coding is used to illustrate the percentage of amino acid types at each position in (C) PxxWxxR (9 sequences) and (D) RxxWxxR peptides (4 sequences).

Figure 2. Analysis of peptide ligand binding. (A) *In vitro* translated, ^{35}S-methionine-labeled, full-length peptides (left, R8-01; right, R8-04) were assayed for binding to immobilized Mth in the presence or absence of various synthesized peptides. Concentrations of the peptide competitors were 30 μM for N-Stunted (N-St) and 10 μM for R8-01 and R8-01 SCR. Bound peptides are expressed in cpm (+ standard deviation, when available) and have been background subtracted with a negative control. (B) Intrinsic tryptophan fluorescence of Mth W120S ectodomain, R8-12 peptide, and their complex upon excitation at 295 nm. (B, inset) Fluorescence titration of 300 nM R8-12 peptide with Mth W120S at an emission wavelength of 345 nm. (C) Fluorescence

spectra of wild-type Mth ectodomain with and without R8-04 peptide upon excitation at 295 nm.

Figure 3. Structure of the Mth ectodomain in complex with the R8-01 15-mer peptide. (left) Ribbon diagram of the Mth ectodomain. Electron density shows the putative peptide binding site from an averaged 3.5 Å $F_O - F_C$ map contoured at 9 σ. (right) Scaled model depicting the full-length structure of Mth (adapted from (*22*)). The transmembrane region is represented by the structure of rhodopsin (*43*). The putative peptide binding site is shown, along with the sequence of the 2nd extracellular loop that contains a partial RWR motif.

Figure 4. Selected peptides recognize the full-length Mth receptor. (A) Fluorescence microscopy of CHO cells transiently transfected with a Mth-GFP fusion construct. Cells expressing Mth-GFP (left) were stained with 150 nM rhodamine-tagged R8-12 (right). (B) Unstained cells, sorted by FACS, exhibited a range of Mth-GFP expression (left). Staining with rhodamine-R8-12 (right) revealed a direct correlation between the level of Mth-GFP expression (X-axis) and the degree of staining (Y-axis). The slight tailing at high GFP levels (left panel) is due to uncompensated crosstalk between the GFP and rhodamine channels.

Figure 5. Selected peptides act as antagonists of Mth signaling. (A) The N-Stunted agonist peptide (20 μM final) was added to HEK-Mth cells pre-incubated with and without the indicated concentration of R8-12 peptide antagonist. Mth activation resulted in intracellular calcium mobilization and enhanced fluorescence. Fluorescence spectra

were divided by a baseline average, calculated from the region of data prior to the addition of N-Stunted. The dashed line indicates a control where only buffer (without agonist) was added. (B) Concentration dependence of the inhibition of Mth signaling by peptides R8-12 and R8-14. Signals were taken at a time point ~13 sec after the addition of 10 μM N-Stunted agonist and are expressed as a fraction of the fluorescence observed in the absence of antagonists.

Figure 6. The scrambled R8-01 peptide acts as a potent agonist for Mth signaling. (A) Comparison of agonist activity between R8-01 SCR and N-Stunted. Fluorescence spectra were measured as in Figure 5A. (B) Concentration dependence of signaling by Mth agonists. Higher concentrations of N-Stunted were not tested due to problems with peptide solubility. Hence, the max fluorescence determined from fitting the R8-01 SCR data was used as a fixed limit for the N-Stunted fit. (C) Concentration dependence of the inhibition of R8-01 SCR-induced Mth signaling by peptides R8-12 and R8-14. Data are reported as in Figure 5B except that the signals were taken at a time point ~7 sec after the addition of agonist.

Figure 7. Minimal peptides for Mth activation. (A) A series of 15-mer peptides derived from N-Stunted were tested for their ability to activate Mth in the cell-based calcium mobilization assay. Reported values (average of two experiments, + standard deviation) represent the maximum fluorescence achieved after the addition of peptide divided by the baseline average. The shaded region highlights the putative minimal peptide agonist. “Blank” is a negative control where buffer without peptide was added. (B) A series of

12-mer peptides were tested as in (A) for the R8-01 SCR agonist. All peptide sequences listed have an additional C-terminal glycine (not shown).

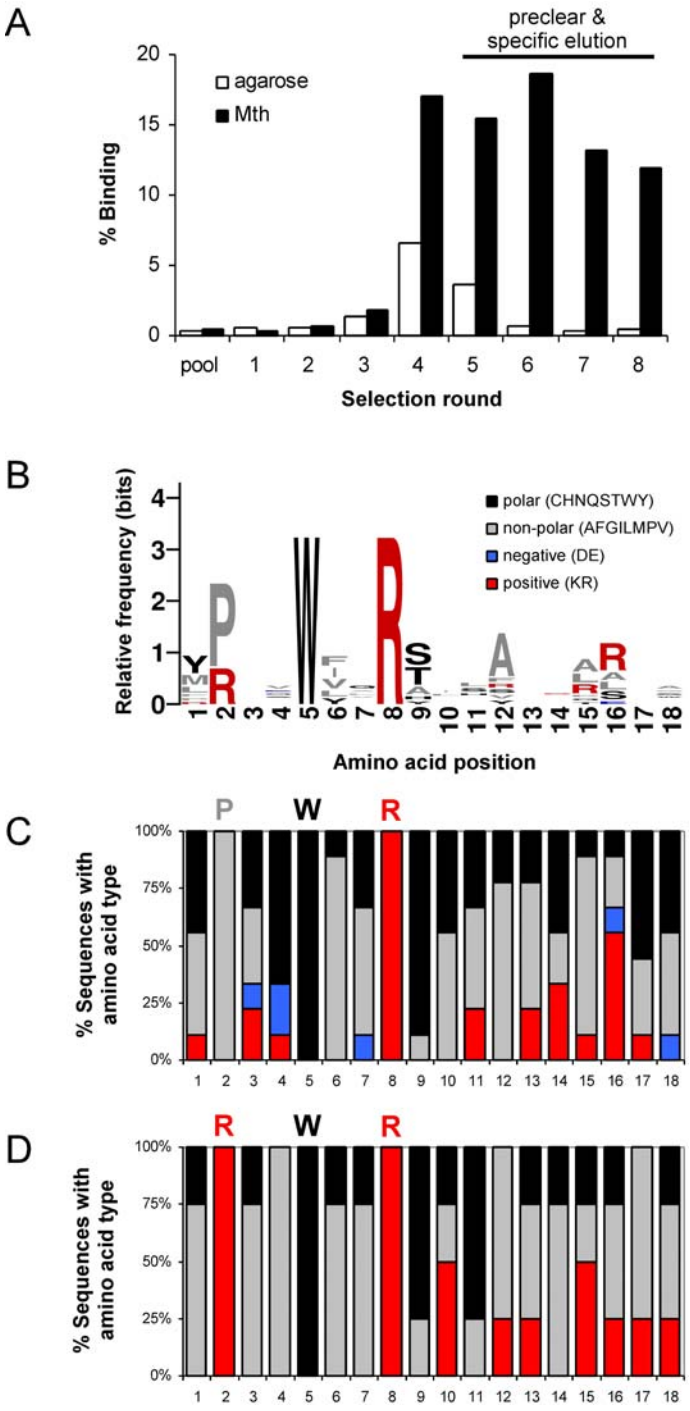
A
preclear &
specific elution
agarose
Mth
% Binding
Selection round
pool
B
Relative frequency (bits)
polar (CHNQSTWY)
non-polar (AFGILMPV)
negative (DE)
positive (KR)
Amino acid position
C
P
W
R
% Sequences with amino acid type
D
R
W
R
% Sequences with amino acid type

Figure 1

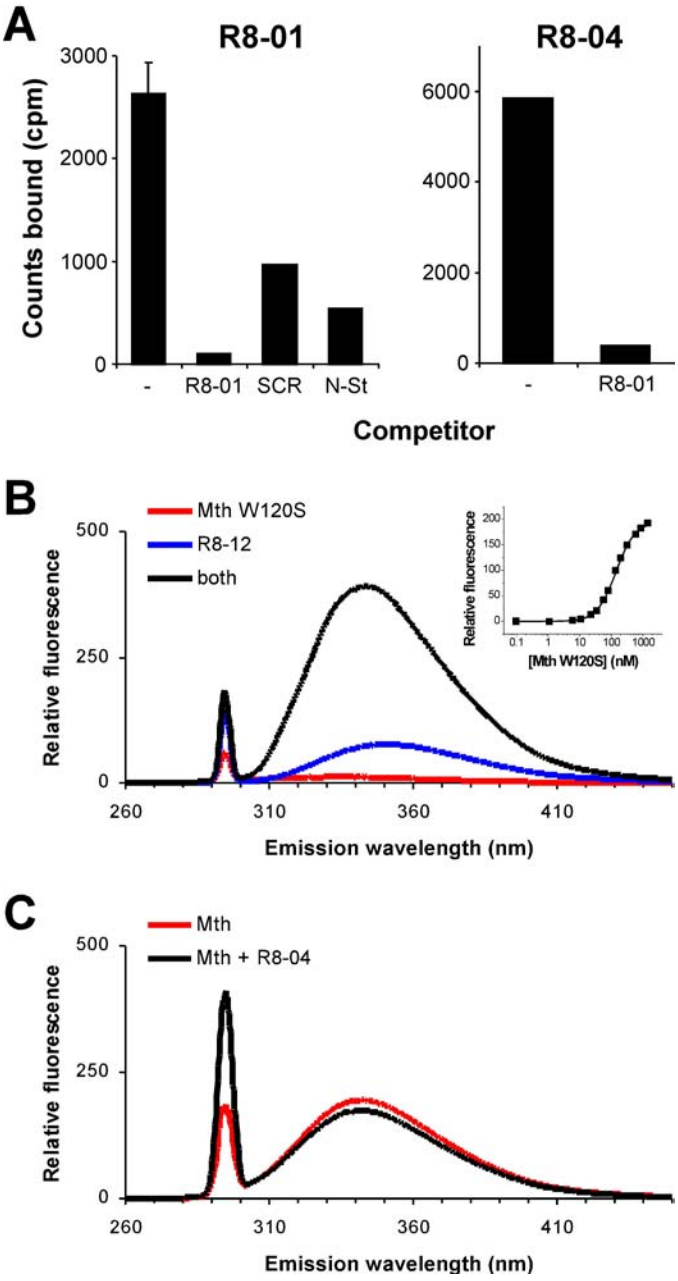
A
R8-01
R8-04
Counts bound (cpm)
3000
2000
1000
0
6000
4000
2000
0
-
R8-01
SCR
N-St
-
R8-01
Competitor
B
Mth W120S
R8-12
both
Relative fluorescence
500
250
0
260
310
360
410
Emission wavelength (nm)
200
150
100
50
0
0.1
1
10
100
1000
[Mth W120S] (nM)
C
Mth
Mth + R8-04
Relative fluorescence
500
250
0
260
310
360
410
Emission wavelength (nm)

Figure 2

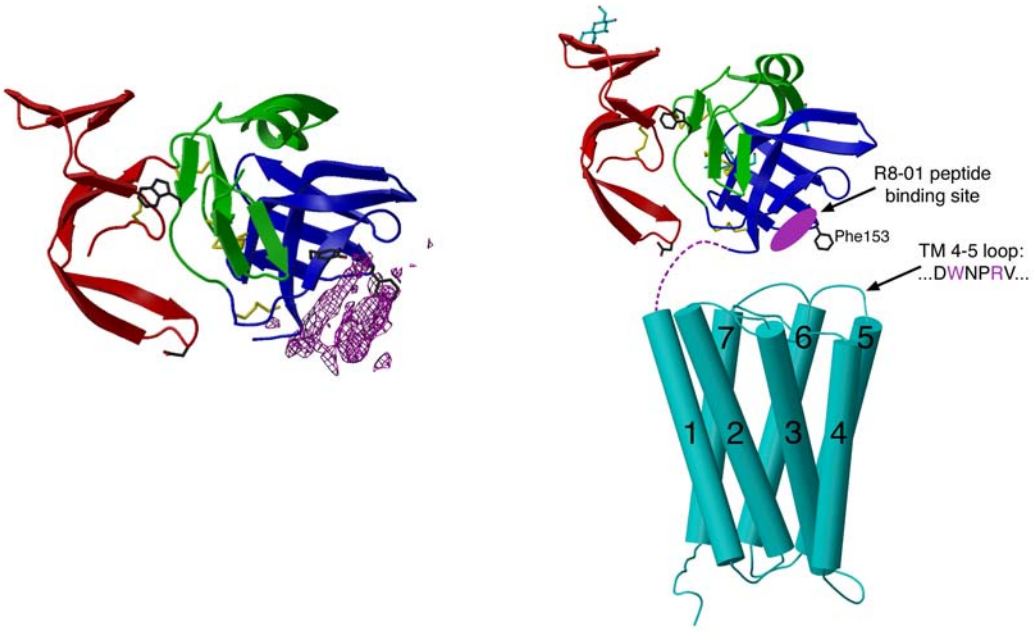

Figure 3

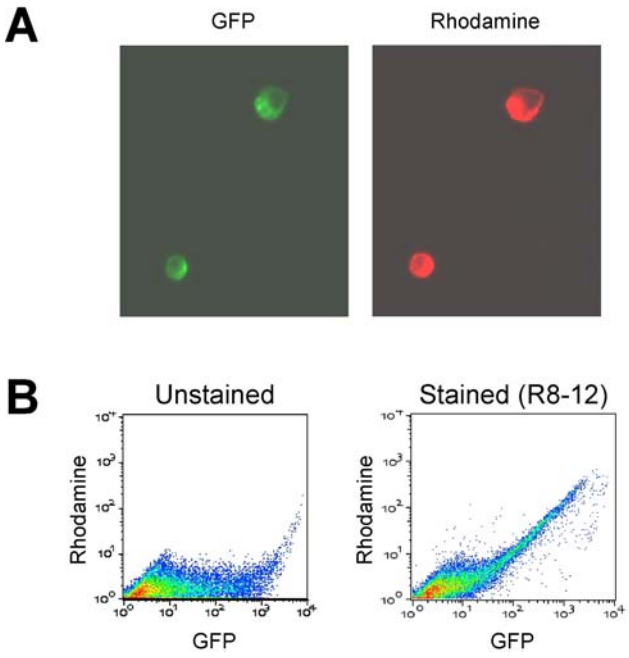
A
GFP
Rhodamine
B
Unstained
Stained (R8-12)
Rhodamine
GFP
Rhodamine
GFP

Figure 4

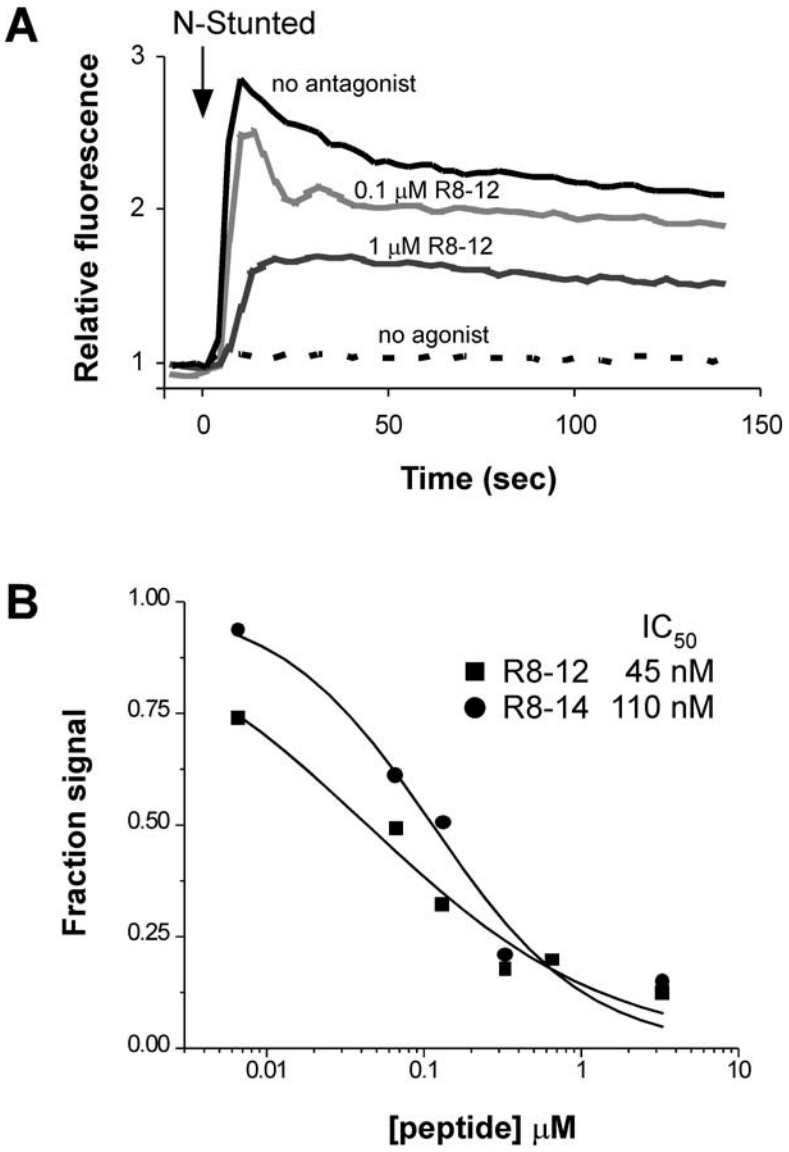
A
N-Stunted
no antagonist
0.1 μM R8-12
1 μM R8-12
no agonist
Relative fluorescence
Time (sec)
B
IC50
R8-12 45 nM
R8-14 110 nM
Fraction signal
[peptide] μM

Figure 5

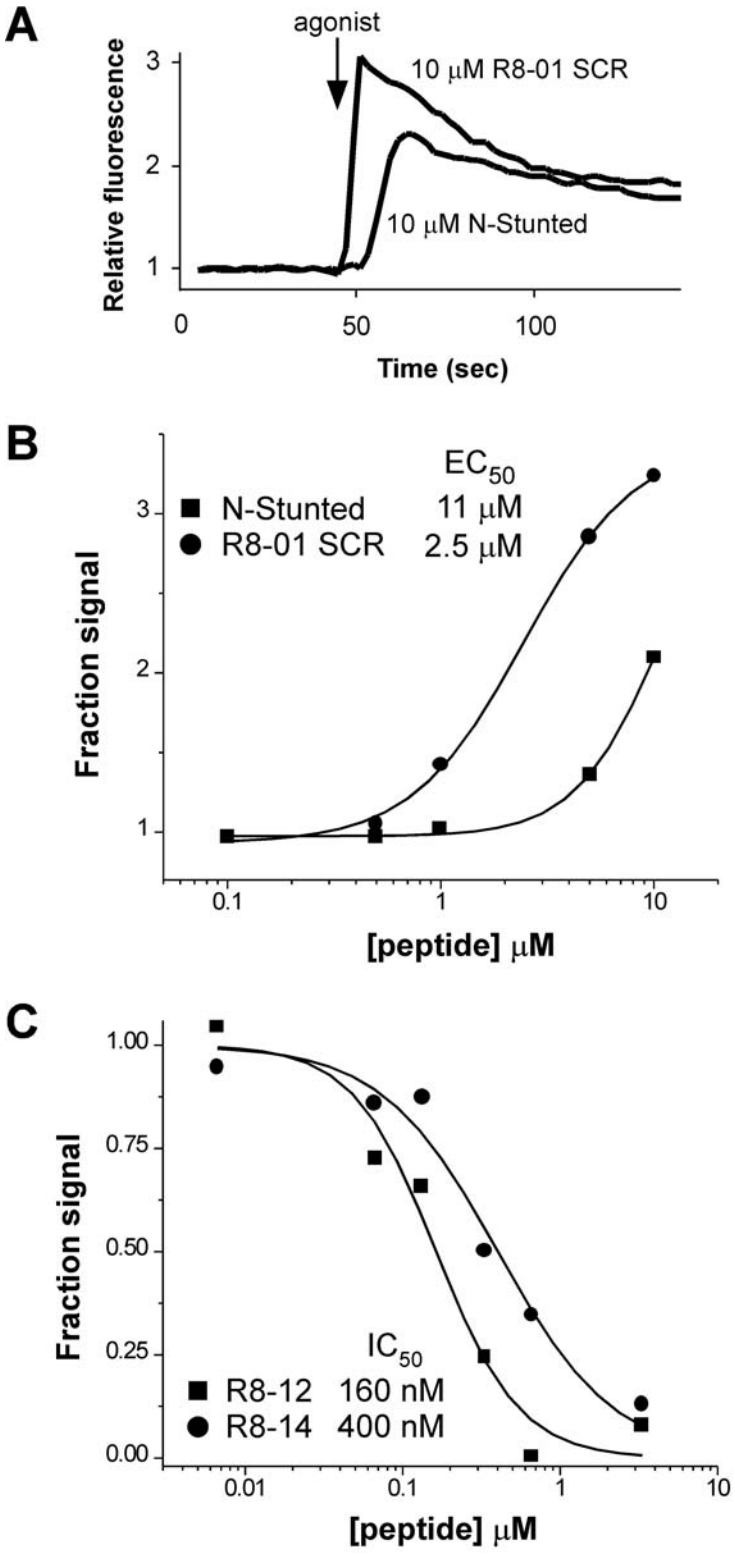
A
agonist
10 μM R8-01 SCR
10 μM N-Stunted
Relative fluorescence
Time (sec)
B
EC50
N-Stunted 11 μM
R8-01 SCR 2.5 μM
Fraction signal
[peptide] μM
C
IC50
R8-12 160 nM
R8-14 400 nM
Fraction signal
[peptide] μM

Figure 6

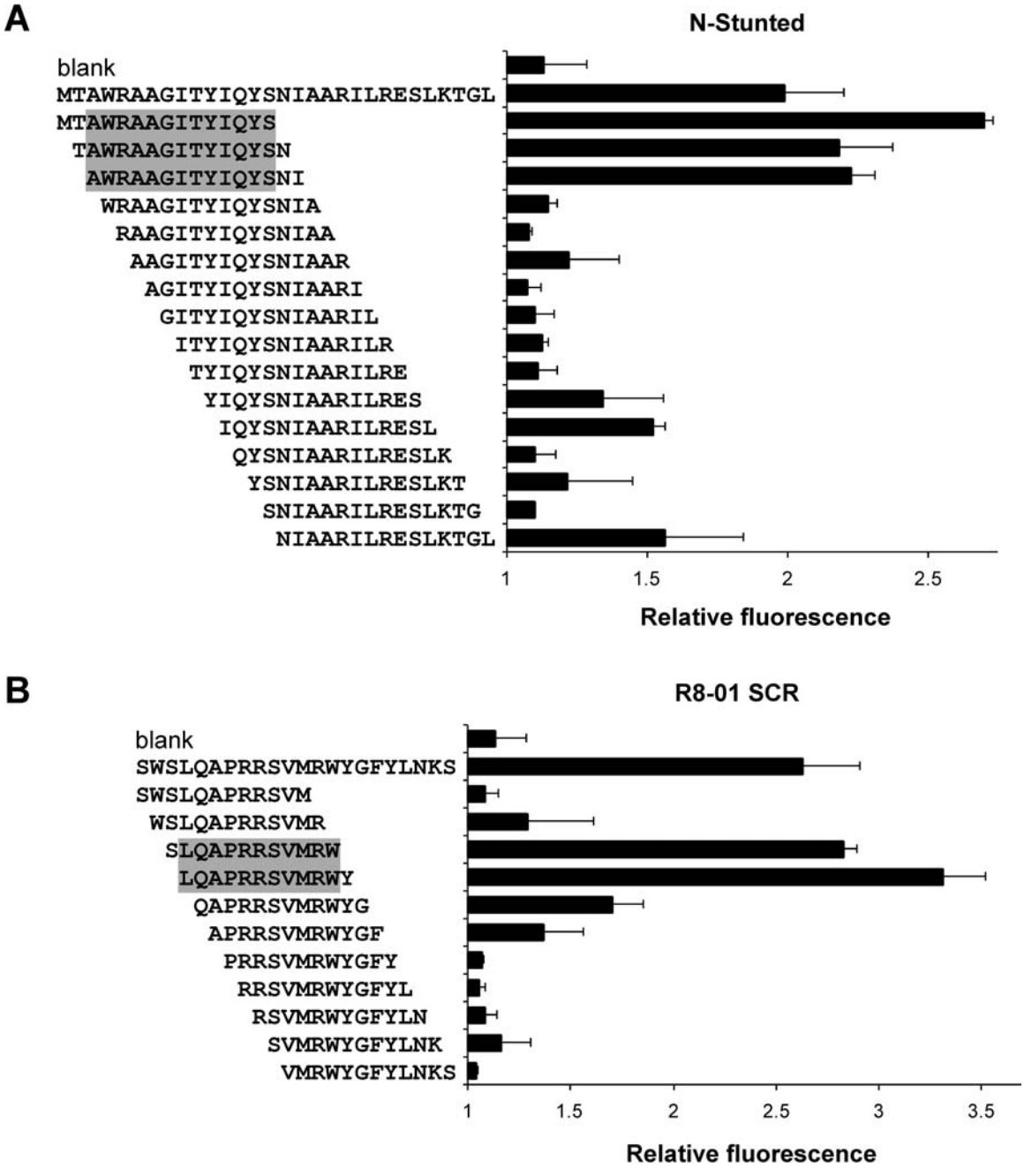
A
N-Stunted
blank
MTAWRAAGITYIQYSNIAARILRESLKTGL
MTAWRAAGITYIQYS
TAWRAAGITYIQYSN
AWRAAGITYIQYSNI
WRAAGITYIQYSNIA
RAAGITYIQYSNIAA
AAGITYIQYSNIAAR
AGITYIQYSNIAARI
GITYIQYSNIAARIL
ITYIQYSNIAARILR
TYIQYSNIAARILRE
YIQYSNIAARILRES
IQYSNIAARILRESL
QYSNIAARILRESLK
YSNIAARILRESLKT
SNIAARILRESLKTG
NIAARILRESLKTGL
1
1.5
2
2.5
Relative fluorescence
B
R8-01 SCR
blank
SWSLQAPRRSVMRWYGFYLNKS
SWSLQAPRRSVM
WSLQAPRRSVMR
SLQAPRRSVMRW
LQAPRRSVMRWY
QAPRRSVMRWYG
APRRSVMRWYGF
PRRSVMRWYGFY
RRSVMRWYGFYL
RSVMRWYGFYLN
SVMRWYGFYLNK
VMRWYGFYLNKS
1
1.5
2
2.5
3
3.5
Relative fluorescence

Figure 7

Supporting Information

Table I. Sequences of selected peptides.[a]

	Clone	Peptide sequence		Frequency
Round 5	R5-01	NQKFSPERFTVWWLRASSALLRVPGLR		2/14
	R5-02	IQLVNMPRVGTLRRANMNMSPWRARCR	*	
	R5-03	RYVWYLRTKHRRSLRLRSACARGSSA	*	
	R5-04	HLFSWRDYPWHWVYRSLLARAPRP		3/14
	R5-05	SSLSPPWPASWSPSRPSAPRAAPSTPT	*	
	R5-07	APRAVWIQRAIQAMFRLASRQESKAFN		
	R5-08	KWLVLGRPVQWFVRTLMAMHQAGGSMI		
	S5-01	SNPKMPSLWLVLLSLHTRNEFPNSVSV		2/14
	S5-04	PKKWIQRHIRALRARTWSYFFLSRTR		
	S5-06	LPLEWFERSSSAAAAASWGRPPRRSG	*	
Round 7	R7-01	IVSWGSFPSSWLQRYYLAKRREADVTL		
	R7-02	VRIGYTSKPGGMNPGNSYTMSIIRMLI		
	R7-03	SSLSPPWPASWSPSRPSAPRAAPSTPT	*	
	R7-05	ELGQFQRLGLPYQWYLRTISYVTFRTA		
	R7-06	VLYPREWFFRAWKSYNASNAGLKDTPR	*	
	R7-07	RSPWARQFPEWDRMRNHMNPI	*	
	R7-08	IYSAYPVSWVARTCAATRARSAGARSA	*	
Round 8	R8-01	NVSWGSFPSSWLQRYYLAKRREADVTL		4/20
	R8-03	GDDMYRIREFLANYRPIWVMRSNLAQL		
	R8-04	VRIGYTSKPGGMNPGNSYTMSIIRMLI		7/20
	R8-07	LKYPDTWLARSLSVFYLRKSARQGKSV		
	R8-12	RLVWIVRSRHFGPRLRMALLGSDRKMW		
	R8-13	ELGQFQRLSLPYQWYLRTISYVSLRTA		
	R8-14	APRAVWIQRAIQAMFRLASRQESKAFN		
	R8-07b	STAGSRARSTSWGTRSPWTWPTPARTG	*	
	R8-08b	SSLSPPWPASWSPSRPSAPRAAPSTPT	*	2/20
	R8-09b	RYVWYLRTKHRRSLRLRSACARGSSA	*	

[a] Only the random region of the peptide library is shown. For peptides that appeared more than once, the frequency out of the total number of clones sequenced for that round is shown. Marked sequences (*) contained deletions or mutations that modified the constant C-terminal peptide (not shown). The sequence for R7-07 assumes that translation started at an alternate methionine codon in the random region, as the originally encoded methionine was followed by several stop codons. Related peptides that appeared in more than one selection round are color-coded.

Supplemental Figure 1. Binding interaction of R8-04 peptide with immobilized Mth ectodomain, measured by SPR. The indicated concentrations of R8-04 peptide were injected (45 mL at 0 s, with a 45 mL/min flow rate) across ~500 RU of immobilized Mth-biotin. The global kinetic fits (black) are overlaid on the original sensorgrams (gray). The derived kinetic parameters are shown in Table III. Sensorgrams have been double-referenced from response curves generated by an appropriate negative control flow cell and averaged buffer blank injections. Three buffer blanks are shown (0 nM R8-04).

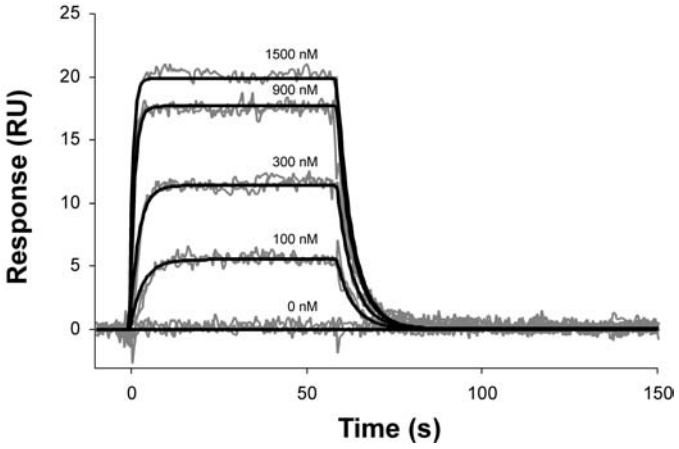

Supplemental Figure 1